Selective synthesis of dimethyl ether on eco-friendly K10 montmorillonite clay

Ali M. Bahmanpour[a], Florent Héroguel[a], Christophe J. Baranowski[a], Jeremy S. Luterbacher[a], Oliver Kröcher[a,b,*]

[a] École Polytechnique Fédérale de Lausanne (EPFL), Institute of Chemical Sciences and Engineering, 1015 Lausanne, Switzerland
[b] Paul Scherrer Institut, Bioenergy and Catalysis Laboratory, 5232 Villigen PSI, Switzerland

ARTICLE INFO

ABSTRACT

The methanol dehydration reaction was studied over environmentally benign, easily accessible and inexpensive K10 montmorillonite clay used as the catalyst at a temperature range between 200–700 °C. Nearly 100% selectivity towards dimethyl ether (DME) at 80% methanol conversion was observed at 300 °C. However, upon heating, the selectivity shifted and the catalyst produced formaldehyde as well as an almost 1:1 M ratio of methane and carbon monoxide at 700 °C. Calcination at 300 °C increased the catalyst acidity due to desorption of chemisorbed water, thereby enhancing the methanol conversion to form DME. Higher calcination temperatures negatively affected the catalyst structure and, therefore, its activity. Catalyst characterization by means of X-ray Diffraction (XRD), X-ray Photoelectron Spectroscopy (XPS), Diffuse Reflectance Infrared Fourier Transform Spectroscopy (DRIFTS), and solid-state Nuclear Magnetic Resonance (MAS NMR) spectroscopy, revealed that the calcination temperature affected the near surface Si/Al ratio as well as the surface hydroxyl groups. It was concluded that the density of the surface Brønsted acid sites is directly proportional to methanol conversion to DME.

1. Introduction

Montmorillonite clay and clay-based materials have attracted much attention as catalysts, due to their natural occurrence, low cost and environmental friendly aspects [1–7]. Moreover, they show a unique combination of characteristics such as high capacity for ion exchange, mesoporosity, both Lewis and Brønsted acidity and a layered structure, which render these aluminosilicates interesting for a broad variety of catalytic reactions. According to this, montmorillonite clay and its acid-treated form (K10 montmorillonite clay) have been found to be active catalysts in many types of reactions such as cationic ring opening polymerization [8,9], esterification [10], acetylation [11], isomerization [12,13] and other reactions [14–17]. As a solid acid catalyst, montmorillonite clay has a great potential to catalyze dehydration reactions [18–20]. Several studies revealed that the activity of montmorillonite clay in specific reactions such as acetalization and esterification is higher compared to zeolites in general, mainly because of the presence of mesopores in the montmorillonite clay structure [21–23]. Another catalytic dimension is added to clays, when used as support for redox-active metals in various reactions [6,24].

Due to the above mentioned high activity of clays for dehydration

reactions in combination with its eco-friendly properties, we have specifically studied the dehydration reaction of methanol over K10 montmorillonite clay (acid-treated montmorillonite clay), because methanol is one of chemical industry's main building blocks and will likely continue to be in the future when it is produced from renewable carbon sources [25]. The focus of the study was on temperatures up to 300 °C, since this is the relevant temperature range for the synthesis of DME from methanol over K10 montmorillonite. However, to investigate the ongoing chemistry and the methanol reaction network on this catalyst, the temperature range up to 700 °C was screened and inspected as well.

DME is a clean alternative fuel for diesel engines and its synthesis has gained much interest recently [26–30]. Low NOₓ emission, negligible smoke formation and non-toxicity of DME make it an attractive inexpensive diesel fuel [31]. DME is also considered as a base material for the synthesis of the alternative diesel fuel, polyoxymethylene dimethyl ethers (OME), by insertion of CH_2O units [32]. A direct DME to OME synthesis method has been claimed [33,34] and further studies are under investigation which, if coupled with methanol dehydration to DME, can create an alternative sustainable method of OME formation directly from methanol in the gas phase. Besides direct applications of

DME such as substitution of diesel fuel by OME, methanol dehydration to DME has garnered further attention since it is the only pathway for the Methanol-to-Olefins (MTO) process [35–37]. Here in this study, we closely examined DME formation as well as the methanol reaction network on the K10 montmorillonite clay surface.

2. Experiments

K10 montmorillonite clay (Sigma–Aldrich) was tested in a fixed bed plug-flow quartz reactor, into which methanol was dosed by saturating the carrier gas argon at T = 30 °C. K10 montmorillonite clay was pelletized, crushed, sieved (250–450 μm) and dried at 120 °C overnight before use. Some of the K10 montmorillonite clay samples were further calcined at different temperatures for 3 h. 200 mg of catalyst were loaded into the reactor and fixed with quartz wool for each run. The quartz reactor was heated using heating wires and a PID temperature controller. The product stream was analyzed quantitatively using an online MATRIX-MG01 FTIR spectrometer (Bruker) equipped with OPUS-GA software and a 10 cm gas cell heated at 120 °C. The catalyst samples, which were calcined before being loaded into the reactor, were first heated at the same calcination temperature for 3 h before changing the temperature back to the operating conditions and introduction of methanol (reagent grade, Merck). The data were collected after 1 h for each experiment. However, experiments were monitored from the beginning to ensure no data is ignored. For reaction network analysis, two temperature cycles were used in order to verify the catalyst stability while collecting data. At each temperature, data were collected as soon as the temperature stabilized. Brunauer-Emmett-Teller (BET) surface and Barrett-Joyner-Halenda (BJH) mesoporous volumes were calculated using N_2-physisorption measurements on a Micromeritics 3Flex apparatus at liquid nitrogen temperature between 10^{-5} and 0.99 relative N_2 pressure. Samples (ca. 100 mg) were dried at 120 °C (temperature reached with a ramp of 2 °C/min) under vacuum ($< 10^{-3}$ mbar) for 4 h and a leak test was performed prior to the analysis. Diffuse Reflectance Infrared Fourier Transform Spectroscopy (DRIFTS) spectra were recorded using a high temperature Harrick DRIFT cell on a Perkin Elmer Frontier spectrometer equipped with a mercury cadmium telluride detector. Spectral intensities were reported in Kubelka-Munk (K-M) units which are based on the Kubelka-Munk function to relate the concentration to the reflected radiation. Spectra were typically collected with 32 scans at a resolution of 4 cm^{-1}. Helium (100 mL/min) was passed through a bubbler filled with pyridine to saturate the samples with pyridine vapor (30 min, 150 °C). Physisorbed pyridine was eliminated by flowing pure helium (30 min, 150 °C) through the cell. Temperature Programmed Oxidation (TPO) was performed on a Micromeritics Autochem 2920 II instrument. The samples (ca. 100 mg) were loaded into a U-shaped cell and dried for 30 min under He flow (50 mL/min) at 150 °C (5 °C/min). After cooling down to 50 °C, the flow was switched to a 2:98 (volumetric ratio) O_2:He mixture and temperature was ramped to 1000 °C (10 °C/min). During this process, CO and CO_2 desorption were monitored using a calibrated thermal conductivity detector as well as MKS Cirrus II mass spectrometer calibrated to mass of 28 and 44.

X-ray Diffraction (XRD) tests were performed using an X'Pert-Pro X-ray diffractometer (Philips) equipped with a Cu-Kα source. The XRD patterns were recorded with the step size of 0.01. X-ray Photoelectron Spectroscopy (XPS) was used to study the near surface structure of the samples. ^{27}Al solid-state Nuclear Magnetic Resonance (MAS NMR) spectroscopy (400 MHz Bruker equipped with a console AVIII HD and a 2.5 mm MAS probe triple channel) was used to study the aluminum coordination of the various samples to examine the potential structural changes.
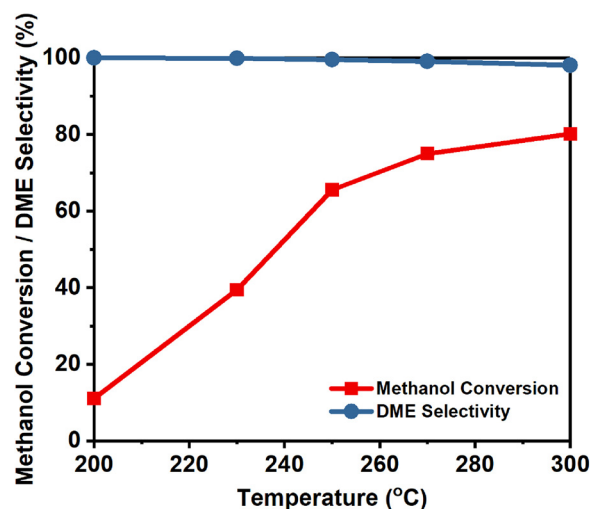

Fig. 1. Methanol conversion and DME selectivity at various temperatures. Catalyst: K10 montmorillonite clay calcined at 300 °C.

3. Results and discussion

3.1. Effect of reaction temperature

Methanol dehydration reaction over K10 montmorillonite clay was studied in the gas phase in the temperature range of 200–300 °C (Fig. 1). At 200 °C, 100% selectivity towards DME was observed. At higher temperatures, methanol conversion increased significantly while selectivity towards DME did not diminish notably. At 300 °C, methanol conversion reached its maximum value with slight deterioration of DME selectivity (due to formation of traces of formaldehyde shown later). This result showed that K10 montmorillonite clay is an active and selective catalyst for DME production from methanol.

In order to find out more about the ongoing chemistry on this catalyst, we inspected the methanol reaction network on K10 montmorillonite clay in the temperature range of 200–700 °C. We observed that very different compositions of the product gas stream were found in dependency of the reaction temperature (Fig. 2). Between 200–300 °C DME was formed with the same selectivity as already displayed in Fig. 1. At 300 °C, traces of formaldehyde were observed which slightly affected DME selectivity. At 400 °C, the same reaction products were observed with a slightly higher content of formaldehyde. As soon as the temperature increased to 500 °C, formation of methane and carbon
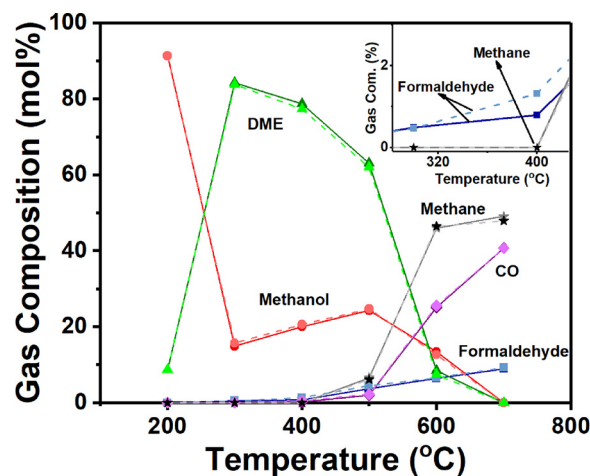

Fig. 2. Effect of reaction temperature on product distribution. Solid line: First temperature cycle, Dash line: Second temperature cycle. Catalyst: K10 montmorillonite clay calcined at 300 °C.

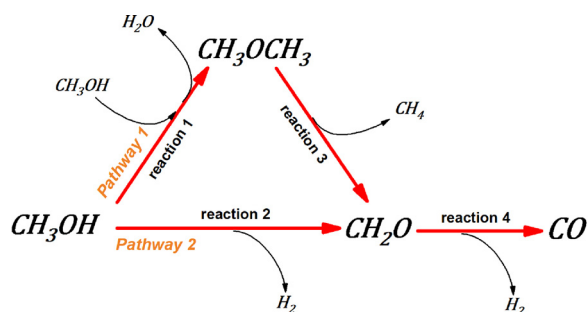**Fig. 3.** Proposed methanol reaction network on K10 montmorillonite clay calcined at 300 °C.

Fig. 4. Arrhenius plot for methanol dehydration reaction to DME. Catalyst: K10 montmorillonite clay calcined at 300 °C.

monoxide as well as a considerable increase in formaldehyde yield were noticed with a simultaneous decrease in DME concentration. The temperature increase led to a further increase of methane, formaldehyde, and carbon monoxide. The effect of temperatures higher than 300 °C on the product distribution was investigated in two independent temperature cycles to verify the stability of the catalyst during the experiment, because the catalyst was calcined at only 300 °C optimized for DME production (discussed later). The results obtained from the two cycles show close match which confirms that the catalyst did not encounter deterioration during this catalytic test.

Considering the observed product gas stream analysis, the methanol reaction network could be divided into two pathways based on the operating temperature (Fig. 3): Methanol dehydration reaction to DME (reaction 1 in Pathway 1) occurred dominantly in the relatively lower temperature range of 200–400 °C. Observation of formaldehyde while no methane was detected (300–400 °C, Fig. 2 inset) means methanol could, in parallel, be directly dehydrogenated to formaldehyde without going through DME (Pathway 2). Based on previous studies, the most likely catalytically active sites in K10 montmorillonite clay for methanol dehydrogenation reaction are sodium ions [38], whose presence were noticed in the catalyst structure (Table S1). Temperature increase to 400 °C promoted formaldehyde formation since the methanol dehydrogenation reaction is thermodynamically favorable at higher temperatures [39]. In the higher temperature range (500–700 °C), fragmentation of DME by proton transfer as well as formaldehyde decomposition governed the catalytic reaction system. The formation of methane as well as the significant decrease of DME yield at 500 °C, seem to imply that the most likely source of methane formation is the occurrence of a fragmentation reaction initiated by proton-transfer (reaction 3 in Pathway 1). Although not observable from the product stream analysis in our study, hydrogenation of the intermediately formed coke could be another source of methane production. At 700 °C, methanol and DME were completely converted to methane and formaldehyde. Formaldehyde, in turn, partially decomposed to carbon monoxide and hydrogen (reaction 4 in Pathway 1 and 2). At very high temperatures in the gas phase, also radical reactions have to be considered. However, non-catalytic methanol dehydrogenation to formaldehyde and partly to CO requires very high temperatures as high as 900 °C, which are beyond the temperature range applied in our study [40].

In the temperature range of 200–300 °C, methanol conversion was far from equilibrium [41]. The Arrhenius plot in Fig. 4 shows the dependency of the reaction rate on the temperature in this region. The activation energy was calculated to be 102 kJ/mol. At 300 °C, the equilibrium conversion was reached and methanol conversion was governed by the thermodynamic limitations of the dehydration reaction.

3.2. Effect of surface acidity

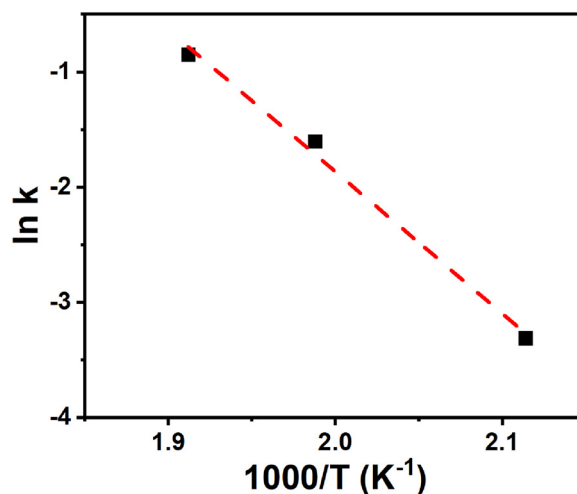Since acidity is reported to be an important factor in alcohol

dehydration reactions [42], the effective performance of the K10 montmorillonite clay as catalyst in methanol dehydration reaction might be attributed to its acidity. The nature of acidity of the K10 montmorillonite clay was examined by FTIR spectroscopy using pyridine adsorption (Fig. S1). After exposure of the sample to excess pyridine vapor at 150 °C, the FTIR spectra of the clay displayed characteristic bands from pyridine adsorbed on both Lewis and Brønsted acid sites ($1453\,cm^{-1}$/$1493\,cm^{-1}$ and $1493\,cm^{-1}$/$1545\,cm^{-1}$, respectively). However, the complete disappearance of the peak at $1545\,cm^{-1}$ at 250 °C showed the low strength of the Brønsted acid sites. Although the catalyst retained some Lewis acidity at 250 °C, these sites also almost disappeared at 350 °C. Considering the high content of chemisorbed water in the K10 montmorillonite clay structure and the effect of water desorption on strengthening the acidity of the clay based on the literature [9,43], we investigated the effect of calcination temperature on the performance of the K10 montmorillonite clay in methanol dehydration reaction. Although physisorbed water desorption occurred during drying process at 120 °C overnight, higher temperatures (200–400 °C) were required for the desorption of chemisorbed water in accordance with literature [44]. The catalysts were calcined at 300 °C, 500 °C, and 700 °C which hereafter are referred to as K10-C300, K10-C500, and K10-C700, respectively. Table 1 shows the BET surface area and the pore volume of the catalysts calcined at different temperatures as well as their activity at 300 °C.

The highest catalyst activity was achieved upon clay calcination at 300 °C. Higher activity of K10-C300 compared to the non-calcined catalyst was expected due to the desorption of chemisorbed water at this temperature which results in the formation of stronger acid sites [45]. In fact, we did not observe desorption of pyridine bonded to both Lewis and Brønsted acid sites at temperatures up to 350 °C by FTIR spectroscopy, attesting the strength of these sites (Fig. 5a). No olefin formation was observed during methanol dehydration reactions despite

Table 1
BET surface area, pore volume and catalyst activity at 300 °C for K10 montmorillonite clay.

Catalyst	S_{BET} (m²/g)	Pore Volume (cm³/g)	Methanol Conversion at 300 °C (%)
K10 montmorillonite clay	221	0.24	70[a]
K10-C300	216	0.26	80
K10-C500	210	0.26	40
K10-C700	188	0.23	6

[a] This value is obtained after 1 h of operation. However, longer reaction time can affect the catalyst and change the value.
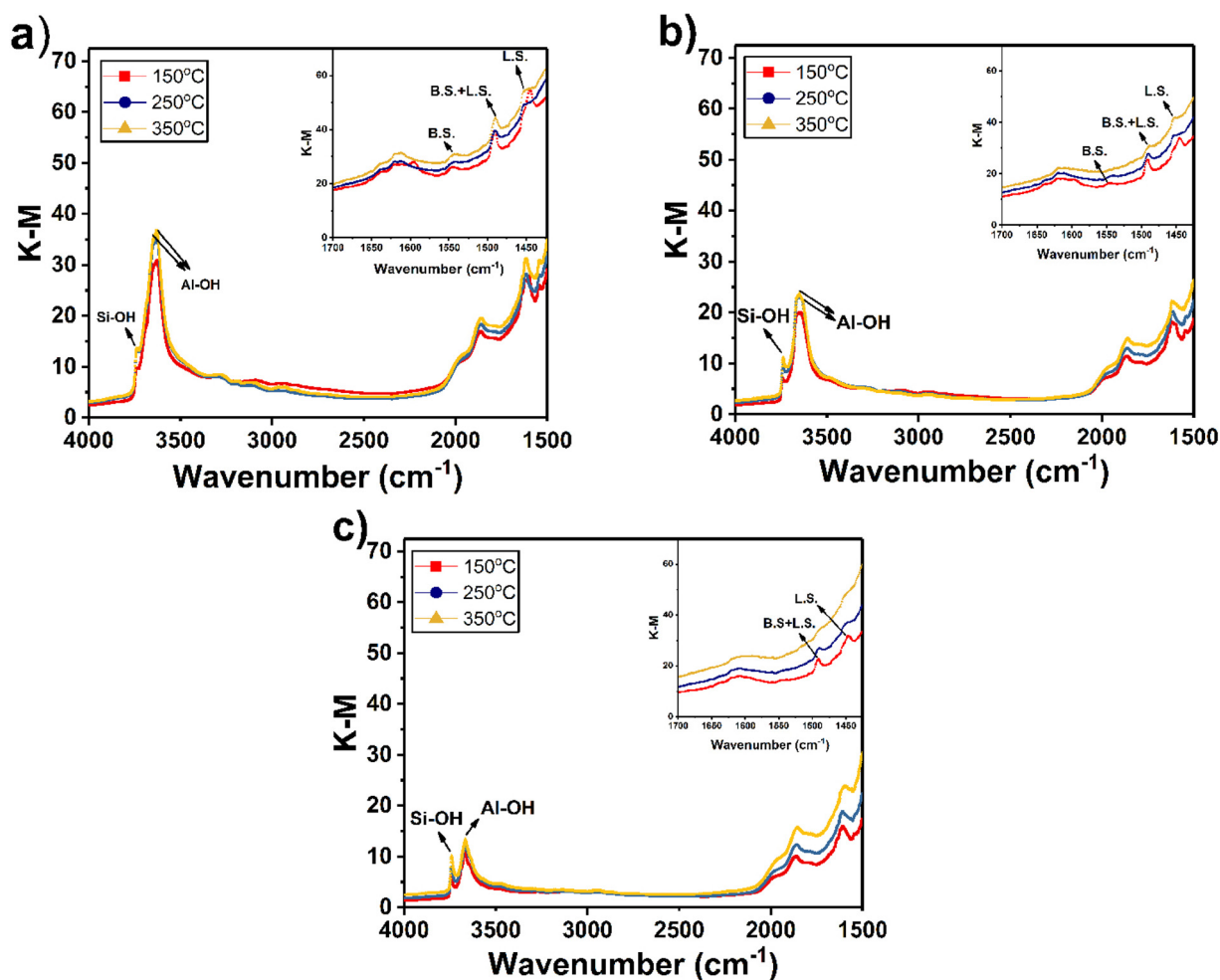
Fig. 5. DRIFT spectra of adsorbed pyridine on a) K10-C300, b) K10-C500 and c) K10-C700 in dependency of the temperature.

the presence of the relatively strong Brønsted acid sites. Potential olefin formation was closely monitored by observing the full IR spectra as well as monitoring the mass balance precision (presented in Fig. S2). Light olefins could form on the catalyst surface during methanol reaction and appear as coke (discussed later). However, it should be negligible considering the fact that no olefin was detected in the gas phase despite the mass balance accuracy. It should be also noted that coke formation due to olefins reaction and deposition is mostly common in alumino-silicate structures with cages and cavities [46,47]. It is claimed in some studies that only Lewis acid sites play the major role in methanol de-hydration [48–50]. Based on these studies, Brønsted acidity leads to the further dehydration of DME to form olefins. Even though our ob-servation is inconsistent with these reports, it may be possible that olefin formation requires still stronger Brønsted acid sites compared to the sites which can be formed through calcination. This explanation is supported by the absence of remarkably strong Brønsted acid sites such as Si-(OH)-Al bonds in K10 montmorillonite clay [51] in contrast to zeolites, over which the formation of olefins has been observed at si-milar reactions conditions [52,53]. FTIR spectroscopy of adsorbed pyridine showed that an increase of the calcination temperature to 500 °C and 700 °C (K10-C500 and K10-C700) resulted in a decrease of the amount and strength of Brønsted and Lewis acid sites (Fig. 5b and c), along with the catalytic activity (Table 1). Therefore, these ob-servations clarify the effect of thermal treatment on the Lewis acidity of K10 montmorillonite clay, which has been debated in the literature [54,55]. It was also noted that for K10-C500 and K10-C700, the in-tensity of the bonds at 3624 cm^{-1} and 3644 cm^{-1} assigned to two forms of Al-OH bonds on the K10 montmorillonite clay surface,

decreased [45,56]. Disappearance of the structural Al-OH bond at 3624 cm^{-1} implies that the structural change of the K10 montmor-illonite clay is due to the calcination. For K10-C700, a significant de-crease of the Al-OH bond was observed which indicates the onset of the dehydroxylation of the K10 montmorillonite clay surface [44]. How-ever, it is important to note that the intensity of the signal at 3745 cm^{-1} assigned to Si-OH [45] did not follow the same trend showing that the Si-OH groups stayed intact. Therefore, it is more likely that Al-OH de-hydroxylation was caused by the structural change of the clay than by mere Al−OH bond break due to the thermal treatment. Therefore, a more detailed study of the catalyst structure was necessary.

3.3. Effect of thermal treatment on catalyst structure

The X-ray Diffraction (XRD) pattern of the catalysts (Fig. 6) revealed that the structure of the K10 montmorillonite clay was affected by the calcination. By acid treatment of the montmorillonite clay to form K10 montmorillonite clay, the layered structure of this aluminosilicate was affected and opened as it can be noticed by the change in intensity of the 001 basal peak (Fig. S3). This also can be noticed by the higher surface area of the K10 montmorillonite clay (221 m^2/g (Table 1)) compared with untreated montmorillonite clay ($\sim$20–40 m^2/g (Sig-ma–Aldrich)) in which the interlayer space is not reachable for N$_2$ molecules [57]. Nevertheless, the two-dimensional lattice of the clay was preserved through the acid treatment, which was confirmed by XRD peaks at 19.8°, 34.9°, and 61.8° assigned to the *hk0* indices of (020,110), (200,130), and (060,330), respectively [58–60]. Upon temperature treatment at 300 °C, the two-dimensional lattice of the clay
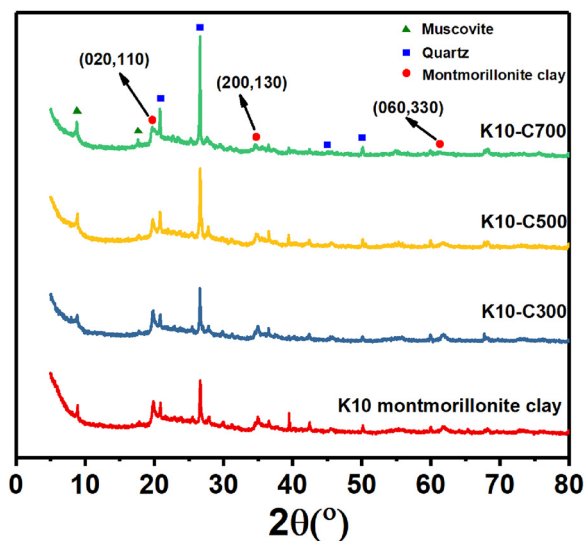
Fig. 6. XRD pattern for K10 montmorillonite clay calcined at various temperatures.

Fig. 7. ^{27}Al MAS NMR for K10 montmorillonite clay calcined at various temperatures.

sheets was still intact although the layered structure was fully lost (Fig. S3). However, it can be noticed from the XRD patterns that higher temperatures of 500 and 700 °C completely destroyed the two-dimensional lattice of the clay. No aluminum crystalline phase was detected by XRD which is most likely attributed to the formation of an amorphous aluminum phase after decomposition of the clay lattice while the silica layer formed quartz (peaks at 21.6°, 26.6°, 45.5°, and 50.1°) [58].

The concentration of various elements near the clay surface after calcination was assessed by X-ray Photoelectron Spectroscopy (XPS). The near surface Si/Al ratios are presented in Table 2 based on the XPS results. The full spectra are presented in Fig. S4. The near surface Si/Al ratio of the K10 montmorillonite clay was measured to be 6.2 for the non-calcined catalyst and 6.8 for K10-C300. This ratio increased for K10-C500 and K10-C700 to 7.8 and 10.9, respectively. This change in the near surface Si/Al ratio combined with the decrease of the intensity of the Al-OH bond shown by IR spectroscopy and the XRD results indicate the loss of aluminum on the surface due to the deformation and decomposition of the two-dimensional lattice of the K10 montmorillonite clay and probably, diffusion of aluminum to the bulk of the K10 montmorillonite clay. This deformation and the rearrangement of aluminum coordination were studied by ^{27}Al solid state NMR spectroscopy (Fig. 7). Although the majority of aluminum is bound in octahedral coordination (considering the structure of montmorillonite clay sheet), tetrahedral coordination can also be observed in the spectra of the non-calcined K10 montmorillonite clay, which is in agreement with previous reports [61]. The aluminum coordination of the samples did not show a significant change for K10-C300, while the proportion of the tetrahedral aluminum increased for K10-C500 and the signal intensity decreased. Upon calcination at 700 °C, the signal intensity of the NMR spectra decreased considerably and the octahedral coordinated

aluminum transformed into other coordination showing formation of a less structured amorphous aluminum phase. This observation confirmed the formation of a less-structured amorphous aluminum phase due to the dehydration and consequently, dehydroxylation of the octahedral layer of aluminum oxide [44,62]. In conclusion, it can be stated that the loss of the Brønsted acidity mainly occurred due to Al−OH bond dehydroxylation, which, in turn, is followed by the deformation and decomposition of the two-dimensional lattice of K10 montmorillonite clay.

The time-on-stream behavior of K10-C300 over 15 h at 300 °C is plotted in Fig. S5. No deactivation was observed during the run and the pore volume of the catalyst was not affected (Fig. S6). However, Temperature-Programmed Oxidation (TPO) revealed coke formation on the catalyst surface during reaction (Fig. S7). As mentioned earlier, a possible source of coke formation might be light olefins produced on the surface of the catalyst. However, since light olefins have not been detected in the gas phase in our experiments, this pathway appears to be rather unlikely, but cannot be excluded. Irrespective of the ongoing chemistry, the formed coke on the catalyst surface did not affect the active sites since the catalyst activity remained stable over 15 h time on stream. Therefore, further coke characterization was not considered in this study.

4. Conclusion

Methanol dehydration reaction to DME was studied over eco-friendly and inexpensive K10 montmorillonite clay. The catalytic activity of this low-cost green catalyst in DME formation (100% selectivity towards DME at 80% methanol conversion) at the temperature range of 200–300 °C makes it an alternative catalytic material for the methanol dehydration reaction. Although coke deposition was detected of the surface of K10 montmorillonite clay during reaction at 300 °C, no catalyst deactivation was observed even after 15 h. Through product gas stream analysis, the methanol reaction network at various temperatures was studied. While selective DME formation was observed at the temperature range of 200–400 °C, the catalyst exhibited high activity for the proton-transfer-induced fragmentation of methanol at 100% conversion as well as the partial decomposition of formaldehyde at high temperatures (600–700 °C). Our findings showed that calcination of the K10 montmorillonite clay at 300 °C for 3 h can enhance the Brønsted acidity of the catalyst which in turn, resulted in higher activity in the DME formation reaction. It was also confirmed that no detectable

Table 2
Near surface Si/Al ratio based on XPS.

Catalysts	Si/Al ratio[a]
K10 montmorillonite clay	6.2
K10-C300	6.8
K10-C500	7.8
K10-C700	10.9

[a] Data obtained based on XPS experiment. Si 2p and Al 2p peaks were used for this quantification. Relative Sensitivity Factor (RSF) used for Si 2p and Al 2p is 0.368 and 0.256, respectively.
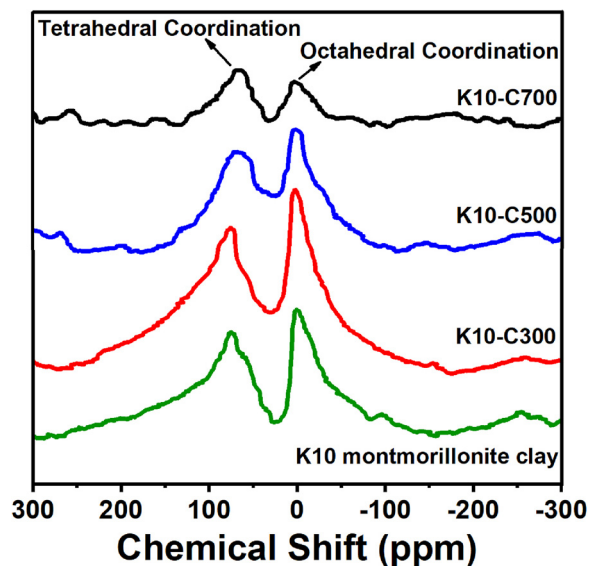
olefin production was observed in the product stream even in the presence of relatively strong Brønsted acid sites on the K10 montmorillonite clay surface which were formed upon calcination. Extensive characterization studies revealed that the disappearance and decrease of the strongly Brønsted-acidic Al-OH groups upon calcination at high temperatures (500–700 °C) was due to the dehydroxylation as well as the phase change of the clay (deformation of the clay two-dimensional lattice) and consequently, absence of aluminum atoms near the catalyst surface.

Associated content

Elemental analysis of K10 montmorillonite clay (Table 1); DRIFT spectra upon adsorption and desorption of pyridine on non-calcined K10 montmorillonite clay (Fig. S1); Gas composition obtained by FTIR and mass balance accuracy. T = 300 °C. Catalyst: K10 montmorillonite clay calcined at 300 °C (Fig. S2); XRD pattern of the Montmorillonite clay, K10 montmorillonite clay, and K10-C300 to show the 001 basal peak assigned to the layered structure of montmorillonite clay (Fig. S3). XPS spectra for K10 montmorillonite clay, K10-C300, K10-C500, and K10-C700 (Fig. S4). Time-on-Stream for methanol dehydration reaction to DME at 300 °C. Catalyst: K10 montmorillonite clay calcined at 300 °C (Fig S5); Comparison of the pore size for fresh and used catalyst after reaction at 300 °C. Catalyst: K10 montmorillonite clay calcined at 300 °C (Fig. S6); TPO for K10-C300, K10-C500 and K10-C700 used at 300 °C. MS signal for total carbon ($CO + CO_2$) vs temperature (Fig. S7) (PDF).

Author contributions

The manuscript was written through contributions of all authors. All authors have given approval to the final version of the manuscript.

Acknowledgments

Appendix A. Supplementary data

Supplementary material related to this article can be found, in the online version, at doi:https://doi.org/10.1016/j.apcata.2018.05.006.

References

[1] A. Rokicińska, P. Natkański, B. Dudek, M. Drozdek, L. Lityńska-Dobrzyńska, P. Kuśtrowski, Appl. Catal. B Environ. 195 (2016) 59–68.
[2] S.P. Chavan, G. Bishwa Bidita Varadwaj, K.M. Parida, B.M. Bhanage, ChemCatChem 8 (2016) 2649–2658.
[3] H. Boukhatem, H. Khalaf, L. Djouadi, F.V. Gonzalez, R.M. Navarro, J.A. Santaballa, M. Canle, Appl. Catal. B Environ. 211 (2017) 114–125.
[4] K. Li, J. Lei, G. Yuan, P. Weerachanchai, J.-Y. Wang, J. Zhao, Y. Yang, Chem. Eng. J. 317 (2017) 800–809.
[5] J. Han, T. Wang, S. Feng, C. Li, Z. Zhang, Green Chem. 18 (2016) 4092–4097.
[6] V.K. Soni, R.K. Sharma, ChemCatChem 8 (2016) 1763–1768.
[7] A.M. Elfadly, I.F. Zeid, F.Z. Yehia, M.M. Abouelela, A.M. Rabie, Fuel Process. Technol. 163 (2017) 1–7.
[8] A. Yahiaoui, M. Belbachir, J. Appl. Polym. Sci. 100 (2006) 1681–1687.
[9] A. Yahiaoui, M. Belbachir, A. Hachemaoui, Int. J. Mol. Sci. 4 (2003) 548–561.
[10] O. Marvi, L.Z. Fekri, M. Takhti, Russ. J. Gen. Chem. 84 (2014) 1837–1840.
[11] K.-I. Shimizu, T. Higuchi, E. Takasugi, T. Hatamachi, T. Kodama, A. Satsuma, J. Mol. Catal. Chem. 284 (2008) 89–96.

[12] S.T. Belt, W.G. Allard, J. Rintatalo, L.A. Johns, A.C.T. Van Duin, S.J. Rowland, Geochim. Cosmochim. Acta 64 (2000) 3337–3345.
[13] B.S. Kumar, A. Dhakshinamoorthy, K. Pitchumani, Catal. Sci. Technol. 4 (2014) 2378–2396.
[14] D. Bahulayan, S.K. Das, J. Iqbal, J. Org. Chem. 68 (2003) 5735–5738.
[15] U.R. Pillai, E. Sahle-Demessie, Appl. Catal. Gen. 245 (2003) 103–109.
[16] M.A. Martinez-Lorente, P. Battioni, W. Kleemiss, J.F. Bartoli, D. Mansuy, J. Mol. Catal. Chem. 113 (1996) 343–353.
[17] U. Flessner, D.J. Jones, J. Rozière, J. Zajac, L. Storaro, M. Lenarda, M. Pavan, A. Jiménez-López, E. Rodríguez-Castellón, G. Busca, J. Mol. Catal. Chem. 168 (2001) 247–256.
[18] H. Zhao, C.H. Zhou, L.M. Wu, J.Y. Lou, N. Li, H.M. Yang, D.S. Tong, W.H. Yu, Appl. Clay Sci. 74 (2013) 154–162.
[19] M.L. Kantam, P.L. Santhi, M.F. Siddiqui, Tetrahedron Lett. 34 (1993) 1185–1186.
[20] C. Krutpijit, B. Jongsomjit, J. Oleo Sci. 65 (2016) 347–355.
[21] B. Thomas, S. Sugunan, J. Porous Mater. 13 (2006) 99–106.
[22] C.H. Zhou, Appl. Clay Sci. 53 (2011) 87–96.
[23] G. Nagendrappa, Appl. Clay Sci. 53 (2011) 106–138.
[24] B.F. Sels, D.E. De Vos, P.A. Jacobs, Catal. Rev. Sci. Eng. 43 (2001) 443–488.
[25] G.A. Olah, A. Goeppert, G.K.S. Prakash, Beyond Oil and Gas: The Methanol Economy, second edition, (2009).
[26] S. Asthana, C. Samanta, A. Bhaumik, B. Banerjee, R.K. Voolapalli, B. Saha, J. Catal. 334 (2016) 89–101.
[27] H. Ham, J. Kim, S.J. Cho, J.-H. Choi, D.J. Moon, J.W. Bae, ACS Catal. 6 (2016) 5629–5640.
[28] C. Zhou, N. Wang, Y. Qian, X. Liu, J. Caro, A. Huang, Angew. Chem. Int. Ed. 55 (2016) 12678–12682.
[29] M. Gentzen, W. Habicht, D.E. Doronkin, J.-D. Grunwaldt, J. Sauer, S. Behrens, Catal. Sci. Technol. 6 (2016) 1054–1063.
[30] K. Takeishi, Y. Wagatsuma, H. Ariga, K. Kon, K.-I. Shimizu, A.C.S. Sustain, Chem. Eng. 5 (2017) 3675–3680.
[31] L. Xinling, H. Zhen, Sci. Total Environ. 407 (2009) 2234–2244.
[32] C.J. Baranowski, A.M. Bahmanpour, O. Kröcher, Appl. Catal. B Environ. 217 (2017) 407–420.
[33] Q. Zhang, Y. Tan, G. Liu, J. Zhang, Y. Han, Green Chem. 16 (2014) 4708–4715.
[34] Q. Zhang, W. Wang, Z. Zhang, Y. Han, Y. Tan, Catalysts 6 (2016).
[35] B.P.C. Hereijgers, F. Bleken, M.H. Nilsen, S. Svelle, K.-P. Lillerud, M. Bjørgen, B.M. Weckhuysen, U. Olsbye, J. Catal. 264 (2009) 77–87.
[36] P. Dejaifve, J.C. Védrine, V. Bolis, E.G. Derouane, J. Catal. 63 (1980) 331–345.
[37] W.W. Kaeding, S.A. Butter, J. Catal. 61 (1980) 155–164.
[38] S. Ruf, G. Emig, Appl. Catal. Gen. 161 (1997) L19–L24.
[39] A.M. Bahmanpour, A. Hoadley, A. Tanksale, Rev. Chem. Eng. 30 (2014) 583–604.
[40] W.-L. Dai, L.-P. Ren, Handb. Heterogen. Catal. (2008).
[41] B.T. Diep, M.S. Wainwright, J. Chem. Eng. Data 32 (1987) 330–333.
[42] R. Rousseau, D.A. Dixon, B.D. Kay, Z. Dohnálek, Chem. Soc. Rev. 43 (2014) 7664–7680.
[43] N. Kaur, D. Kishore, J. Chem. Pharm. Res. 4 (2012) 991–1015.
[44] N. Garg, J. Skibsted, J. Phys. Chem. C 118 (2014) 11464–11477.
[45] D. Liu, P. Yuan, H. Liu, J. Cai, D. Tan, H. He, J. Zhu, T. Chen, Appl. Clay Sci. 80–81 (2013) 407–412.
[46] J.H. Kang, R. Walter, D. Xie, T. Davis, C.-Y. Chen, M.E. Davis, S.I. Zones, ChemPhysChem 19 (2018) 412–419.
[47] M.A. Deimund, L. Harrison, J.D. Lunn, Y. Liu, A. Malek, R. Shayib, M.E. Davis, ACS Catal. 6 (2016) 542–550.
[48] C. Wang, X. Ma, Q. Ge, H. Xu, Catal. Sci. Technol. 5 (2015) 1847–1853.
[49] D.R. Van der Vaart, Research Triangle Institute, United States. Environmental Protection Agency, Catalytic Dehydration of Methanol: Phase I, Final Report, U.S. Environmental Protection Agency, 1988.
[50] A.A. Rownaghi, F. Rezaei, M. Stante, J. Hedlund, Appl. Catal. B Environ. 119–120 (2012) 56–61.
[51] S. Bodoardo, F. Figueras, E. Garrone, J. Catal. 147 (1994) 223–230.
[52] Z. Jia, D. Cai, Y. Cui, W. Qian, F. Wei, Catal. Today 301 (2018) 244–247.
[53] H. Schulz, Catal. Today 154 (2010) 183–194.
[54] D.R. Brown, C.N. Rhodes, Catal. Lett. 45 (1997) 35–40.
[55] T. Cseri, S. Békássy, F. Figueras, S. Rizner, J. Mol. Catal. Chem. 98 (1995) 101–107.
[56] Z.B. Molu, Y. Seki, K. Yurdakoç, Polym. Bull. 64 (2010) 171–183.
[57] K. Bahranowski, A. Gaweł, A. Klimek, A. Michalik-Zym, B.D. Napruszewska, M. Nattich-Rak, M. Rogowska, E.M. Serwicka, Appl. Clay Sci. 140 (2017) 75–80.
[58] P.J. Wallis, W.P. Gates, A.F. Patti, J.L. Scott, E. Teoh, Green Chem. 9 (2007) 980–986.
[59] G.W. Brindley, London, Crystal Structures of Clay Minerals and Their X-Ray Identification, Mineralogical Society, 1980.
[60] L. Le Forestier, F. Muller, F. Villieras, M. Pelletier, Appl. Clay Sci. 48 (2010) 18–25.
[61] T. Shinoda, M. Onaka, Y. Izumi, Chem. Lett. 24 (1995) 495–496.
[62] I.W.M. Brown, K.J.D. MacKenzie, R.H. Meinhold, J. Mater. Sci. 22 (1987) 3265–3275.